

Ground state of the atomic structure of $\text{YBa}_2\text{Cu}_3\text{O}_{6+x}$

A. A. Aligia

Centro Atómico Bariloche, 8400 Bariloche, Argentina

H. Bonadeo

*División Física del Sólido, Comisión Nacional de Energía Atómica,
avenida del Libertador 8250, 1429 Buenos Aires, Argentina*

J. Garcés

Centro Atómico Bariloche, 8400 Bariloche, Argentina

(Received 20 February 1990; revised manuscript received 30 May 1990)

We study the ordering of O atoms in $\text{YBa}_2\text{Cu}_3\text{O}_{6+x}$ using a two-dimensional Ising model. We assume a screened Coulomb repulsion between any two O ions of the CuO_x planes, but the interaction between second-neighbor O ions with a Cu ion in between is reduced by a factor f due to charge-transfer effects. We construct the symmetry-independent atomic configurations, which enable us to compare the energy of a large number of structures. We obtain a rich x - f phase diagram that for screening lengths larger than $\sim 1 \text{ \AA}$ and low values of f contains structures compatible with all the diffraction patterns so far observed. The ground state consists of structures composed of linear CuO chains for $f < 0$, or x near 0.5 and $f < 1$, while for $f = 1$ simple lattices of nearly hexagonal symmetry of O ions or vacancies added to the $x = 1$ structure dominate.

I. INTRODUCTION

An important feature of the high- T_c superconductors resides in the subtle changes in the superconducting temperature T_c caused by small compositional variations.^{1,2} It is of crucial importance to determine to what extent these changes are related to modifications in the atomic structure, since the understanding of this phenomenon could lead to the development of stable or metastable materials with higher T_c .^{3,4}

In $\text{YBa}_2\text{Cu}_3\text{O}_{6+x}$, as x is varied, the plateaus in T_c (Ref. 2) and the number of carriers deduced from Hall measurements⁵ are observed. On the other hand, structures that differ in the arrangement of O atoms in the CuO_x planes⁶ were reported to exist for different values of x at low temperatures. The simplest ones are the tetragonal phase for $x = 0$ and the orthorhombic phase for $x = 1$ (Ref. 6). For $x = \frac{1}{2}$, the unit cell is doubled.^{7,8} More complex structures were observed for $x = \frac{1}{8}$ (Refs. 9 and 10), $x = \frac{7}{8}$ (Refs. 10 and 11), x near $\frac{3}{5}$ (Ref. 12), and x near $\frac{2}{3}$ (Ref. 13). The latter two and those of $x = 1$ and $\frac{1}{2}$ are composed of linear Cu-O chains. For brevity we shall call them CS (for "chain structures"). At present, there is controversy over which of these structures are stable and which of them are metastable. From their observations and by comparison with other systems, Alario-Franco *et al.*¹⁰ suggest that a family of different stable ordered phases may be a better representation of the system. Reyes-Gasga *et al.*,¹⁴ by cooling at constant stoichiometry, find that the phase of $x = \frac{1}{2}$ is stable, while other CS seem to be metastable. However, evidence of phase separation into $x \sim 0.7$ and $x = 1$ (Refs. 15 and 16) and into 0.55 and 0.75 (Ref. 17) point towards the stabi-

ty of another phase, at least, between $x = \frac{1}{2}$ and 1.

Most theoretical treatments of the ordering of O atoms are based on an Ising model for one of the CuO_x planes. These planes of variable O content are those perpendicular to the c axis that bisect the shortest Ba-Ba distance.⁶ The parameters of these models were chosen according to two different points of view: (1) two or three arbitrary parameters of magnitude equal to or less than 0.1 eV (Refs. 18–23), and (2) comparatively large screened Coulomb repulsions.^{24,25} In addition to the $x = 0$ and 1 phases (which are easy to explain), the first point of view was used to obtain the $x = \frac{1}{2}$ structure as the ground state for the corresponding composition,¹⁹ and to explain the high-temperature thermodynamics,^{18,20–23} although the good fit of the phase diagram is rather fortuitous.²³ The existence of other chain structures has been proposed to come from spinodal decomposition.²⁶ Partial ordered CS were obtained in recent Monte Carlo calculations.^{27,28} In any case, these theories cannot explain the observed diffraction patterns for $x = \frac{1}{8}$ and $\frac{7}{8}$, which have been shown to be consistent with the second point of view.^{24,25} The following facts point towards the Coulomb repulsion being dominant: (a) the number of carriers is very low,⁵ suggesting a screening length of several \AA (Ref. 29), (b) the variations of the lattice parameters and distances between atoms with x are explained in terms of Coulomb energies,^{30,31} (c) the crystal structure and parameters of $\text{YBa}_2\text{Cu}_3\text{O}_{6+x}$ and La_2CuO_4 are explained very well using empirical atom-atom potentials that include Coulomb interactions,³¹ (d) it is practically impossible to increase x from 1, suggesting a very large nearest-neighbor O-O repulsion,³² (e) the observed structures for $x = \frac{1}{8}$ and $\frac{7}{8}$ (Refs. 9–11) show that the O-O interactions are still im-

portant at distances of order of 11 Å, (f) considering only the Madelung energy, several important properties of this and other high- T_c compounds can be explained,^{33–35} and (g) direct³⁶ and constrained density-functional^{37,38} calculations give values between 1 and 3 eV for the Coulomb repulsion U_{pd} between electrons in nearest-neighbor Cu and O atoms.

The shortcoming in the works of Refs. 24 and 25 is that they cannot reproduce the observed CS for $x = \frac{1}{2}$, x near $\frac{3}{5}$, and x near $\frac{2}{3}$ (which were not known by the authors). However, this drawback is removed if the effects of the Cu-O electronic repulsion U_{pd} and Cu-O charge transfer are also taken into account. Using a modification appropriate to CuO_x planes of an extended two-band Hubbard model that leads to excitonic pairing in CuO_2 planes^{39,40} (and also in BiO_3 systems,^{40,41}) we have shown that these effects lead to a tendency of the system to order in chains, which competes with the direct O-O repulsion.⁴² In the next section we will present a simple argument to show that this tendency can be accounted for by reducing the second-neighbor O-O repulsion if a Cu is in between. Combining exact results in finite clusters and perturbation theory in the hopping, it was shown^{42,43} that the above-mentioned extension of the two-band Hubbard model explains not only the tendency to order in chains, but also the metal-insulator transition at $x = \frac{1}{2}$ (Refs. 5, 44, and 45), the hole count in CuO_2 planes,⁵ and the number of Cu and O holes.⁴⁶

Using the model described in the next section, the main features of the thermodynamics are also reproduced,^{42,47} but there is an important difference with the results obtained using the above-mentioned first point of view due to the larger magnitude of the Coulomb interactions: the tetragonal phase almost avoids occupancy of nearest-neighbor O-O atoms (as suggested earlier^{30–32}). This considerably reduces its energy at a low cost of entropy for $x = \frac{1}{2}$, leading to a comparatively low orthorhombic-tetragonal transition temperature T_0 and to important

correlations of the latter phase, which recalls to mind the $x=1$ orthorhombic structure.^{42,47} The following facts provide evidence of such correlations: (a) direct perturbed-angular-correlation measurements,⁴⁸ (b) there is a discontinuity in the slope of the resistivity versus x curve at $x=0.5$ (probably associated with the metal-insulator transition^{5,44,43}), but no change of slope at T_0 (Ref. 45), and (c) ^{18}O diffusion experiments⁴⁹ show no break in the Arrhenius plot at T_0 .

Here we show that, using a screened Coulomb O-O repulsion, reduced for second neighbors if a Cu ion is in between, all the observed diffraction patterns can be explained. The model is described by essentially two parameters: the screening length λ and the reduction factor f . The model is equivalent to a planar Ising model with interactions of range λ , all antiferromagnetic, i.e., competing if $f > 0$ (x and the O chemical potential μ play the role of the magnetization M and magnetic field B , respectively). Therefore, it is of intrinsic interest in addition to its relevance for high- T_c systems.

The model and the method used to solve it are described in Secs. II and III, respectively. Section IV contains the results, Sec. V, the comparison with experiment, and Sec. VI, a discussion. A short summary of the results has been presented earlier.⁴²

II. MODEL

We call n_i (0 or 1) the atomic occupation number at position i of the sublattice of all possible O positions of the CuO_x plane. We assume that this lattice is square, i.e., we neglect the small orthorhombic distortion and take the lattice parameter $b=a$. Calling ϵ_0 the binding energy of a single O atom of the plane of interest, the Hamiltonian can be written in the form

$$H = \epsilon_0 \sum_i n_i + \frac{1}{2} \sum_{i,j} V_{ij} n_i n_j, \quad (1)$$

where

$$V_{ij} = \begin{cases} V_b = f \frac{A}{b} e^{-b/\lambda} & \text{if } |\mathbf{R}_i - \mathbf{R}_j| = b, \text{ with } \frac{\mathbf{R}_i + \mathbf{R}_j}{2} = \text{Cu position,} \\ \frac{A}{|\mathbf{R}_i - \mathbf{R}_j|} e^{-|\mathbf{R}_i - \mathbf{R}_j|/\lambda} & \text{otherwise} \end{cases} \quad (2)$$

A is a constant of order $\sim e^2$ if real rather than formal charges are used.⁵⁰ In real systems, Cu-O covalency⁵⁰ and the promotion of holes to O atoms as x is increased should decrease A . The screening length λ should also decrease with x , particularly after $x = \frac{1}{2}$ due to the increase in the number of carriers.^{5,43} This is confirmed by oxygen K soft-x-ray emission measurements.⁵¹ Both effects decrease the derivative of the free energy with respect to x , i.e., the O chemical potential. Here we take parameters independent of x . The ground state depends only on x , λ , and f . The fact that $f < 1$ in $\text{YBa}_2\text{Cu}_3\text{O}_{6+x}$ is a consequence of Cu-O charge transfer, Cu intra-

atomic and Cu-O interatomic electronic repulsions.^{42,43} A simple argument can be given for $x \leq \frac{1}{2}$: let us assume first that all O ions are $2-$. For $x=0$, all Cu ions of the CuO_x plane [Cu(1) in the notation of Ref. 6] are $1+$, the rest are $2+$ (Refs. 46 and 52). When O atoms are added, they take the electrons from the highest coordinated Cu(1) ions to minimize the Cu-O nearest-neighbor interaction U_{pd} (Cu^{3+} is almost forbidden because of intraatomic correlations⁵³). If the added x O atoms do not have common nearest-neighbor Cu ions (right-hand side of Fig. 1), they take the electrons from their $2x$ nearest-neighbor threefold-coordinated Cu(1) ions [we remind the

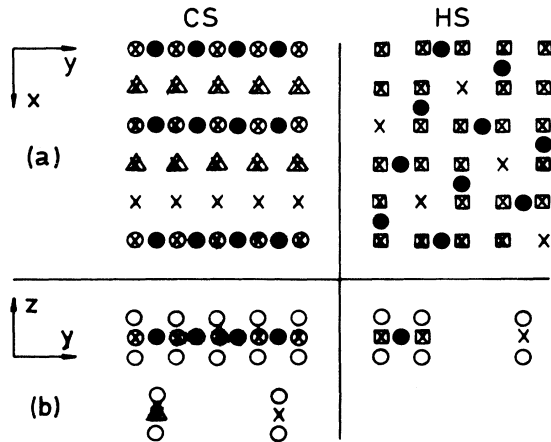


FIG. 1. (a) Scheme of the distribution of holes in the CuO_x planes that result from nearest-neighbor interatomic repulsion U_{pd} , if covalency is neglected and O is presented only as O^{2-} , for two different types of structures. (b) Structural units composed of Cu(1) and its nearest-neighboring O ions contained in planes perpendicular to the CuO_x ones. The meaning of the different symbols is as follows: solid circles, O ions of the CuO_x planes; open circles, O(4) in the notation of Ref. 6; crosses, $[\text{Cu}(1)]^+$; crosses inside triangles, squares, and circles denote $[\text{Cu}(1)]^{2+}$ with coordination 2, 3, and 4, respectively. For CS half the $2x$ holes brought by the x O atoms of the CuO_x planes are in fourfold-coordinated Cu^{2+} ions (with energy gain $-8U_{pd}$) and the other x holes are in twofold-coordinated Cu^{2+} (energy gain $-4U_{pd}$). For the other structures the $2x$ $[\text{Cu}(1)]^{2+}$ ions are threefold coordinated and the total nearest-neighbor Coulomb energy is the same ($-12 \times U_{pd}$). The energy of the CS decreases when holes leave the twofold-coordinated Cu^{2+} atoms due to covalency (see text and Refs. 42 and 43).

reader that each Cu(1) ion always has two bridging out-of-plane O(4) neighbors,⁶ see Fig. 1(b)]. When two O ions have a common Cu neighbor (left-hand side of Fig. 1), the latter is fourfold coordinated and an extra energy $2U_{pd}$ in comparison to threefold coordination is gained when an electron is taken from it. If all O ions were $2-$, since there are not enough Cu ions with more than two nearest-neighbor O ions, another electron should be taken from a two-fold-coordinated Cu ion and the energy gain is lost. The situation comparing infinite CuO chains with disperse structures for $x = \frac{2}{5}$ is illustrated in Fig. 1. For only two added O ions in the planes, there are four threefold-coordinated Cu ions if these O ions do not have a common Cu neighbor. In the other case there is one fourfold- and there are two threefold-coordinated Cu(1) ions. Thus, there should be a twofold-coordinated Cu^{2+} . However, when covalency is taken into account, the twofold-coordinated Cu ion remains nearly $1+$ or intermediate valent at the expense of O holes in O(4) atoms or CuO_2 planes and this results in an energy gain ΔE . This energy should be subtracted from the direct O-O screened Coulomb repulsion to obtain the effective interaction V_b of Eq. (2) (Ref. 42). The value of ΔE depends strongly on model parameters, particularly on the

Cu-O repulsion U_{pd} of the extended two-band Hubbard model. Realistic calculations,^{42,43} which also explain other electronic properties, give values of the order of 1 eV.

A similar argument could be used to argue that the first-neighbor O-O repulsion is also reduced by ΔE . However, this repulsion is so large³⁰⁻³² that, in any case, nearest-neighbor O atoms are avoided in the ground state.

III. METHOD OF SOLUTION

Due to the nature and large number of relevant interactions in our model, the method of geometrical inequalities⁵⁴ and the cluster method,⁵⁵ which are, in general, useful in finding the ground state of Ising models, are not suitable for our case. Monte Carlo calculations^{25,27,28} present difficulties at low temperatures: the "simulated annealing" procedure is characterized by extremely slow kinetics and complete ordering is almost never obtained.^{25,28} For these reasons Monte Carlo methods were used to justify some of the observed structures as transient or metastable, with the dubious assumption that the Glauber or Kawasaki dynamics chosen has some similarity with the O dynamics in the real system.

In view of the above-mentioned difficulties, we have directly compared the energy of a large number of configurations. This method was used earlier in $\text{YBa}_2\text{Cu}_3\text{O}_{6+x}$ (Ref. 19). In our case the studied configurations include all the so far observed or proposed superstructures. Also, since the computer time increases with the number of relevant interactions, which, in turn, increases quadratically with the screening length λ , it was necessary to reduce all possible configurations to those which are not equivalent by symmetry. Otherwise the calculation would have had to be restricted to $\lambda \ll a$ or a much lower number of configurations. Disregarding the structures with nearest-neighbor O atoms, which are obviously unfavorable for $x \leq 1$, the set of calculated structures include the following subsets: (a) all structures whose unit cell or a multiple of it is a rectangle of largest side $\leq 3a$ and area $\leq 8a^2$, (b) all structures with a unit cell $1 \times n$, i.e., those composed of full and empty chains (CS) for $1 \leq n \leq 8$, (c) all simple lattices of O ions with $x \geq \frac{1}{8}$, and (d) all structures with $\frac{1}{2} \leq x \leq \frac{7}{8}$ formed substructuring simple lattices of O ions from the $x=1$ structure. To obtain one and only one representative of all structures that are equivalent by symmetry, we used a group-theoretical method developed by one of us for finite clusters,⁵⁶ which was expanded to take into account periodic boundary conditions. It can be briefly described by the following steps: (1) one of the possible unit cells considered is chosen, (2) the set of all possible O sites of the unit cell is divided into subsets which are generated by application of the point-group G operations to a site, (3) within each subset, all nonequivalent subconfigurations C_i are constructed, (4) from all subconfigurations C_i and C_j belonging to two different subsets, all the possible subconfigurations of the union of both subsets are obtained only once combining C_i and gC_j , where g is one operation representative of those of a double coset in the

$G_i \setminus / G_j$ double coset decomposition^{56(a)} of G (G_k is the symmetry group of the subconfiguration C_k), (5) the procedure is iterated until all subsets are considered, and (6) structures that are equivalent due to translational symmetry to previous ones are disregarded. To illustrate the power of the method, note that, for a unit cell $2\sqrt{2} \times 2\sqrt{2}$ (with 16 possible O positions), there are $2^{16} = 65\,536$ possible configurations. We find that only 997 are nonequivalent and after disregarding those with nearest-neighbor O atoms, only 35 structures remain.

It might happen that the ground state for particular values of the parameters is out of the set of structures we have considered. We believe that if this were the case for not too large screening lengths, the ground-state structure and its energy would be very similar to our result and would not change the trends of our conclusions. This is the case of the structure of Fig. 4(b), which we included because we suspected that it should have lower energy than a similar 2×3 structure. The difference of energy was actually very small. Our cluster-variation method calculations^{42,47} at very low temperatures detected an unexpected ground-state structure only in one case ($x=0.5$, $\lambda=1$, $f=0.6$), but this was a consequence of cutting off the interactions beyond the fifth O neighbors.

IV. RESULTS

For an arbitrary value of x , the ground state of the system is found to consist of a mixture of two phases with two neighboring compositions x_i, x_{i+1} with $x_i < x < x_{i+1}$, that correspond to two structures i and $i+1$. These structures can be classified into four different types represented in Figs. 2–5, respectively. Briefly they can be identified as (1) “chain” structures (CS), (2) nearly

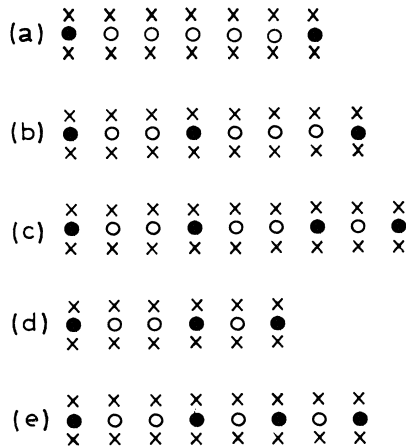


FIG. 2. Unit cells of structures of minimum energy for given composition x , among those composed of full and empty CuO chains (CS). Crosses denote Cu atoms, solid circles represent O atoms, and open circles denote vacant O sites, which, if filled, complete the structure for $x=1$. (a) Example for $x=1/n$ with $n=6$, (b) $x=2/7$, (c) $x=3/8$, (d) $x=2/5$, and (e) $x=3/7$. The corresponding structures for compositions $1-x$ are obtained by interchanging solid and open circles.

“hexagonal” structures (HS), (3) “pair” (or small-chainlet) structures (PS), and (4) others. In the wide region of parameters studied, types 1 and 2 are the most frequent and type 4 is very rare. In the following we explain this classification in more detail.

(1) CS: structures of minimum energy among those of unit cell $1 \times n$ (composed of full and empty chains) and composition $x = m/n$ with m and n integers (see Fig. 2). Khachatryan and Morris proposed similar structures to be originated in spinodal decomposition.²⁶ They are the ground state for f large and negative.

(2) HS: as found earlier by Aligia, Rojo, and Alascio,^{24,25} these structures predominate for $f=1$. They

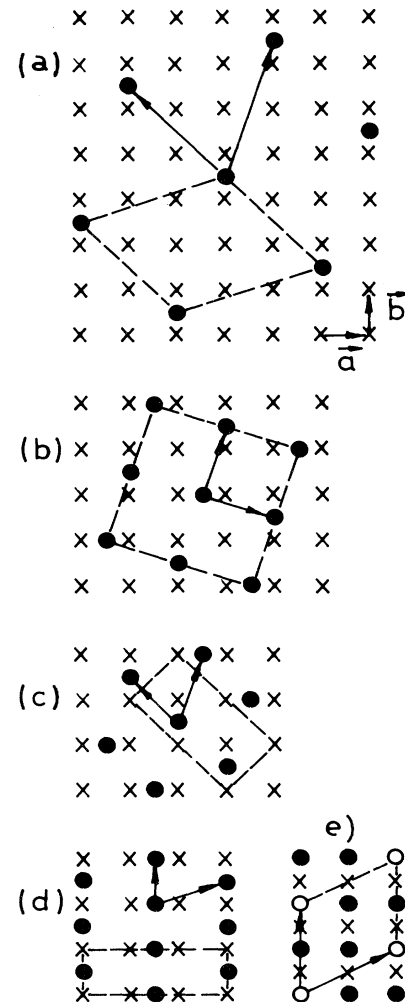


FIG. 3. Examples of structures of minimum energy for given O composition among those built with a simple sublattice of O atoms, or O vacancies on the $x=1$ structure (HS). (a) $x=1/8$, (b) $x=2/5$, (c) $x=1/2$, (d) $x=2/3$, and (e) $x=3/4$. Symbols as in Fig. 2. The basic vectors that define the structure according to Table I are indicated. Dashed lines show a possible choice of unit cell.

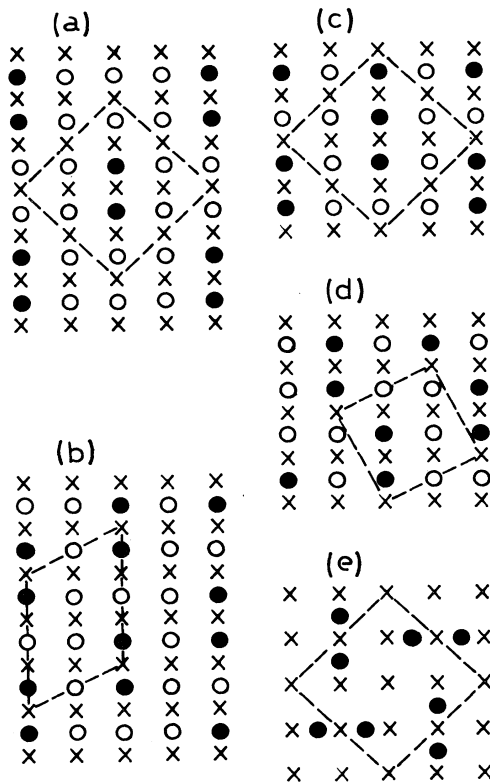


FIG. 4. Structures denoted by PS in the text, which are the ground states of the system for particular values of the parameters: (a) $x = \frac{1}{4}$, (b) $x = \frac{1}{3}$, (c) $x = \frac{3}{8}$, (d) $x = \frac{2}{5}$, and (e) $x = \frac{1}{2}$. Symbols as in Fig. 2. By interchanging solid and open circles in (a)–(d), the corresponding structures for compositions $1-x$ are obtained.

can, in turn, be divided into two groups: (a) For $x \leq \frac{2}{3}$ and $x = 1$, structures of minimum energy among the simple lattices of O ions for a given composition [see Figs. 3(a)–3(d)]. These structures are, in general, the smallest possible deformation of a perfect hexagonal simple lattice (type $p6m$) with the same O concentration. This hexagonal structure would minimize the energy if the O ions could be placed in any position of the plane instead of a square lattice. It also reminds the vortex structure of

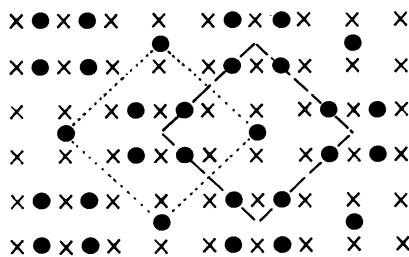


FIG. 5. Ground state of the system for $\lambda = 4a\sqrt{2}$, $f = 1$, and $x = \frac{5}{8}$. Dashed and dotted lines show possible choices of the unit cell. Symbols as in Fig. 2.

type-II superconductors⁵⁷ and, in fact, when the positions of the vortices are restricted to a lattice, structures of this type are predicted⁵⁸ for magnetic fields corresponding to $x = \frac{2}{5}$, $\frac{2}{3}$, and 1 [Figs. 3(b) and 3(d) correspond to Figs. 1(a) and 1(b) of Ref. 58]. The basic vectors of the O lattice define the structure. These vectors are listed in Table I. Note that, for most of these structures, at least one of the basic vectors contains a or b a half-integer number of times. This means that, as far as the main diffraction peaks are concerned,²⁴ these structures would be identified as “tetragonal.” The $x = 1$ structure can also be classified as a CS. (b) For $\frac{2}{3} < x < 1$, structures of minimum energy for a given composition, among those obtained adding a simple lattice of O vacancies to the $x = 1$ structure. The fact that the latter is a square lattice implies that these structures have the same form as in (a).²⁴ In fact, it can be shown that if A is a simple lattice of O ions, B is any O structure built on this lattice and $A-B$ is the structure obtained from A subtracting the O atoms in the positions of B , the energy per unit cell of $A-B$ can be calculated as

$$e_{A-B} = \frac{x_A - 2x_B}{x_A} e_A + e_B \quad (3)$$

Therefore, for fixed A and x_{A-B} , minimizing e_{A-B} reduces

TABLE I. Basic vectors that define (a) for $x \leq \frac{2}{3}$ or $x = 1$, the O lattices of minimum energy, and (b) for $\frac{3}{4} < x < 1$, the structures of minimum energy among those obtained adding a simple lattice of O vacancies to the $x = 1$ ground state (see Fig. 3). The unit vectors are $(1,0) = \mathbf{a}$, $(0,1) = \mathbf{b}$ [Fig. 3(a)]. In case (b), interchanging \mathbf{a} and \mathbf{b} a different structure with the same energy (within our model) is obtained.

x	\mathbf{V}_1	\mathbf{V}_2
$\frac{1}{8}$	(1,3)	(-2,2)
$\frac{2}{15}$	(3,5)/2	(3,-5)/2
$\frac{1}{7}$	(3,5)/2	(5,-1)/2
$\frac{2}{13}$	(1,5)/2	(5,-1)/2
$\frac{1}{6}$	(-1,5)/2	(5,-1)/2
$\frac{2}{11}$	(1,2)	(5,-1)/2
$\frac{1}{5}$	(1,2)	(2,-1)
$\frac{2}{9}$	(1,2)	(3,-3)/2
$\frac{1}{4}$	(1,2)	(2,0)
$\frac{2}{7}$	(1,2)	(3,-1)/2
$\frac{1}{3}$	(0,2)	(3,-1)/2
$\frac{2}{5}$	(1,3)/2	(3,-1)/2
$\frac{1}{2}$	(1,3)/2	(-1,1)
$\frac{2}{3}$	(0,1)	(3,1)/2
$\frac{3}{4}$	(2,1)	(0,2)
$\frac{4}{5}$	(2,1)	(1,-2)
$\frac{5}{6}$	(2,2)	(1,-2)
$\frac{6}{7}$	(3,1)	(1,-2)
$\frac{7}{8}$	(3,1)	(2,-2)
1	(0,1)	(1,0)

to minimizing e_B . An example of this structure is shown in Fig. 3(e) and the basic vectors of these structures for $x \leq \frac{7}{8}$ are given in Table I.

(3) PS: these structures appear at the threshold of stability between CS and HS. In general, they are built from pairs of second-neighbor O atoms (or O vacancies added to the $x=1$ structure) with a Cu in between (see Fig. 4). In two cases [Fig. 4(c)] the basic unit of the structure is the shortest linear chain containing three O atoms (or the O atoms replaced by vacancies). Some structures of these type were proposed by Alario-Franco *et al.*¹⁰ the structures of Fig. 4(a) are the same as those of Fig. 3(c) and 3(g) of Ref. 10. Similarly, our Fig. 4(c) corresponds to Figs. 3(d) and 3(f) of Ref. 10.

(4) In the range of parameters investigated ($f \leq 1$, $\lambda \leq 10a_0$, where $a_0 = a/\sqrt{2}$ is the lattice parameter of the O sublattice), we found only three structures that do not belong to the previously described types. The most frequent of them is the one shown in Fig. 5. Another one is built adding vacancies to the structure of Fig. 3(c), suggesting a generalization of the constructing procedure used for type 2(b) [see Fig. 3(e)] for large λ . The three structures appear only for large values of λ and $f \sim 1$. This is due to the fact that, within our model with constant A and screening length λ , for a given composition, segregation into neighboring phases also implies a segregation of ionic charges. As the screening by mobile carriers is reduced (λ is increased), this segregation becomes energetically unfavorable and the system prefers structures with increasingly larger unit cell and composition nearer to the given one. To accurately describe the academically interesting regime $\lambda \gtrsim 10a_0$ and $f \sim 1$, a larger number of possible structures have to be considered.

In Fig. 6, we show the x - f phase diagram for different values of λ . The regions $0 < x < \frac{1}{8}$ and $\frac{7}{8} < x < 1$ are empty because we have not considered structures with these compositions. The phase diagram is dominated by CS and HS. The transition from one type of structure to the other for a given composition happens at values of f which roughly correspond to the equality between V_b [see Eq. (2)] and the largest interaction between O atoms (or additional vacancies if x is larger than $\frac{2}{3}$) different from V_b in the corresponding HS. The value of this interaction decreases for $x \rightarrow 0$ or $x \rightarrow 1$ and is maximum for $x = \frac{1}{2}$ (compare the length of the basic vectors different from $\pm \mathbf{b}$ in Fig. 3). This explains that, for intermediate values of f , the CS are stable within an interval of values of x which has its midpoint around $x = \frac{1}{2}$. For some values of f , the only stable CS is the one with $x = \frac{1}{2}$. The above-mentioned interval grows with decreasing f . The transition between CS and HS is mediated by PS: when the first two have the same energy, the latter is usually the ground state. This is not apparent in Fig. 6 for x near $\frac{1}{8}$ or $\frac{7}{8}$ because, in these cases, the size of the unit cell of the PS is larger than the maximum size which we have considered in our set of structures.

For different values of λ the same qualitative behavior is obtained (compare the three parts of Fig. 6). As λ increases, two main effects can be observed: (a) The values

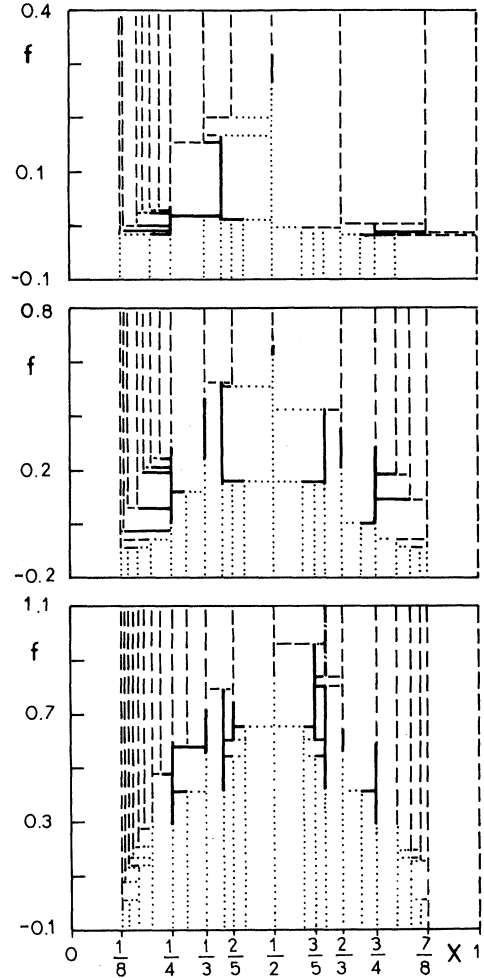


FIG. 6. Ground state of the system as a function of composition x and reduction factor f of the repulsion between second-neighbor O ions with a Cu in between, for different values of the screening length λ : top, $\lambda = 0.4a_0$; middle, $\lambda = a_0$; bottom, $\lambda = 4a_0$, where $a_0 = a/\sqrt{2}$ is the minimum distance between two possible O positions. The structures are uniquely determined by their type (denoted by different lines) and composition. Dotted line, CS (Fig. 2); dashed line, HS (Fig. 3 and Table I); solid line, PS (Fig. 4); and dotted-dashed line, Fig. 5. The structure for $x=1$ can also be classified as a CS.

of f for which the transition between CS and HS takes place increase. This can be understood on the basis of the rough explanation of the transition given above. (b) The number of different structures increases due to the larger cost of energy involved in the segregation of ionic charges, as explained above.

V. COMPARISON WITH EXPERIMENTS

From the density of carriers,⁵ one expects a screening length $\lambda \sim 2a_0$, where $a_0 = a/\sqrt{2}$ for $\text{YBa}_2\text{Cu}_3\text{O}_7$ and increasing for decreasing x . An exaggerated lower bound

for λ is $\sim 0.4a_0$ (Ref. 29). The reduction factor of the second-neighbor O-O interaction with a Cu in between f is more difficult to estimate due to the sensitivity of $\Delta E = (1/f - 1)V_b$ to the electronic parameters,⁴³ and the uncertainty on the exact values of the O charges, but one expects $0 \lesssim f < 1$. Thus, Fig. 6 covers a fairly realistic range of parameters. The fact that, in real systems, A and λ decrease with x , and f also varies, affects the relative stability of the different phases against segregation, but the trends are clear: stable "chain" structures are expected for compositions around $x = \frac{1}{2}$. The most stable CS is the experimentally observed^{7,8} for $x = \frac{1}{2}$. Some authors suggest that it would be the only stable CS (apart from the $x = 1$ phase).¹⁴ Instead, for x near 0 or 1, the structures shown in Fig. 3 (HS) dominate for most values of f . The structure shown in Fig. 3(a) and that obtained from it replacing the O atoms by vacancies added to the $x = 1$ structure, are consistent with the experimental observations for $x = \frac{1}{8}$ and $\frac{7}{8}$ of a unit-cell multiple of $2\sqrt{2} \times 2\sqrt{2}$ (Refs. 9–11). The slightly different structures proposed in these works [basic vectors (2,2) and (2,-2) instead of those of Table I or Fig. 3(a)] have a slightly higher energy (for example, the difference is $2.7 \times 10^{-4} A/a_0$ for $\lambda = 10a_0$, $6.6 \times 10^{-5} A/a_0$ for $\lambda = a_0$, and $6.0 \times 10^{-7} A/a_0$ for $\lambda = 0.4a_0$) and could be favored at moderate temperatures since a greater entropy is expected.

Concerning the observed CS for x near $\frac{2}{3}$, the stability of which is currently under debate, our results for sufficiently low values of f predict stable structures that are quite consistent with the experimental observations, in particular, for $x = \frac{2}{3}$ (Ref. 13) and $x = \frac{3}{5}$ (Ref. 12). For the latter composition, the predicted CS has the unit cell shown in Fig. 2(d). In addition to the main diffraction peaks of the primitive unit cell,²⁴ this structure should present less intense peaks at wave vectors $(m/5, 0, 0)$ in units of $2\pi/a$, with the intensity for $m = 2, 3$ being 6.86 times larger than for $m = 1, 4$, which is consistent with the observed diffuse streaking.¹² Note, however, that the CS for the similar compositions $\frac{4}{7}$ and $\frac{5}{8}$ [Figs. 2(e) and 2(c)] would produce diffraction patterns difficult to distinguish from the previous ones within the experimental resolution. As shown in Fig. 7, a mixture of equal quantities of the three structures, oriented in parallel, produces

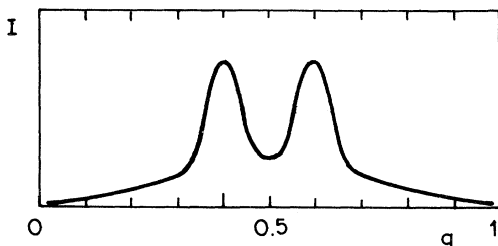


FIG. 7. Diffraction pattern of a mixture of equal parts of in parallel oriented CS (see Fig. 2) with $x = \frac{4}{7}$, $\frac{3}{5}$, and $\frac{5}{8}$, along the $(q, 0, 0)$ direction, excluding the peaks at $q = 0$ and 1 in units of $2\pi/a$. All peaks have been broadened with a half-width of 0.03.

a diffraction pattern very similar to the experimentally observed.¹²

For CS, a $1 - x$ dependence of the number of Cu^+ is expected.^{43,46,52} Thus, the x-ray absorption experiments of Ref. 46, together with the structural evidence,^{7,10,59} suggest a transition from HS to CS at $x \sim 0.35$ for increasing x . This fact can be used to determine f and then a change from CS to HS near $x \sim 0.7$ is predicted neglecting the x dependence of the parameters. In fact, a new jump in the amount of Cu^+ at this value of x has been reported,⁶⁰ and several experiments suggest a phase transition.^{15–17} Also, a minimum in the resistivity^{2,45} and changes in the temperature⁶¹ and O pressure^{32,62} dependence of x are observed.

In the comparison with experiment one should take into account that the structural properties are determined by the number of O atoms in the relevant planes, while the number of holes in the structure is determined by the total number of O atoms per unit cell, and the metal-insulator transition and other properties depend on both quantities.^{42,43} The differences between both O concentrations and the nominal O content are affected by O present in grain boundaries and near surfaces and interfaces⁶³ and by some loss of bridging O(4) atoms⁶⁴ especially for low values of x .

VI. DISCUSSION

We have studied a two-dimensional Ising model to represent the possible oxygen positions of the CuO_x planes of $\text{YBa}_2\text{Cu}_2\text{O}_{6+x}$, which are the relevant ones for the structure. We have assumed a screened Coulomb interaction between any two O ions,^{24,25} but that between second-neighbor interactions with a Cu ion in between was reduced by a factor $f < 1$. We have given a simple argument to show that this reduction factor is due to charge-transfer effects induced by Cu-O Coulomb repulsion. The fact that $f < 1$, the hole count, the metal-insulator transition at $x = 0.5$ and the number of Cu^+ are qualitatively explained in Ref. 43 and briefly in Ref. 42 using the same extended Hubbard model that leads to excitonic pairing in CuO_2 planes.^{39,40}

For realistic values of the screening length λ and a range of positive but small values of f , all the so far observed diffraction patterns^{6–13} can be explained in terms of the ground state of the model for the compositions $x = 0, \frac{1}{8}, \frac{1}{2}, \frac{3}{5}$ (or some mixture of $\frac{4}{7}, \frac{3}{5}$, and $\frac{5}{8}$), $\frac{2}{3}, \frac{7}{8}$, and 1. Models based on arbitrary, comparatively smaller parameters^{18–23} cannot account for the experimental observations at $x = \frac{1}{8}$ and $\frac{7}{8}$. In addition, since these models contain interactions up to second-nearest neighbors only, they predict, at most, three stable structures (for $x = 0, \frac{1}{2}$, and 1). In order to explain a diffraction pattern like the one shown in Fig. 7, even considering metastable phases,⁶⁵ repulsions between O ions at distances $2a$ or larger should be included. Otherwise there is no reason why three consecutive Cu(1)-O(1) chains should be avoided and only one peak centered at $q = 0.5$ is obtained in scattering experiments.⁶⁶ No matter how small these repulsions at distances $2a$ are, they stabilize the CS with

$x = \frac{1}{3}$ and $\frac{2}{3}$ at zero temperature. Similarly, repulsions at larger distances stabilize the other CS shown in Fig. 2 for sufficiently small f . Thus, even for $f = -1$ and in the (unphysical) limit $0 < \lambda \ll a$, the predictions of our model and that of Refs. 19, 21–23, 27, and 28 are different at low enough temperatures. Evidence in favor of the dominant role of Coulomb energies was summarized in the Introduction. Note that estimations of the magnitude of the O-O interactions based on the x dependence of O desorption rates⁶⁷ or of the O chemical potential^{68,69} are actually underestimations because A and λ in Eq. (2) decrease with x , since the concentration of carriers and the number of O holes increase in the metallic phase.^{5,43,51}

Results presented elsewhere^{42,47} using the nine-point approximation of the cluster-variation method, show that, for $x = \frac{1}{2}$ and temperatures much lower than the

nearest-neighbor O-O interaction, the system undergoes a transition to a highly correlated tetragonal phase. There is experimental evidence of these correlations.^{45,48,49} At higher temperatures the transition takes place for $x \sim 0.65$ almost independently of the temperature⁴⁷ in reasonable agreement with experiment.⁶ Thus, the most important aspects of the structural and electronic properties of these systems can be accounted for, at least qualitatively, in terms of strong interatomic correlations.

Note added. After submission of this paper we learned about the electron diffraction patterns obtained by Beyers *et al.*⁷⁰ They are in excellent agreement with our CS for $x = \frac{1}{2}, \frac{3}{5}, \frac{5}{8},$ and $\frac{2}{3}$. We also received a preprint of A. G. Khachatryan, S. V. Semenovskaya, and J. W. Morris, who study a similar model with the method of concentration waves.

-
- ¹J. B. Torrance, Y. Tokura, A. I. Nazzari, A. Bezing, T. C. Huang, and S. S. P. Parkin, *Phys. Rev. Lett.* **61**, 1127 (1988).
- ²R. J. Cava, B. Batlogg, C. H. Chen, E. A. Rietman, S. M. Zahurak, and D. Werder, *Phys. Rev. B* **36**, 5719 (1987).
- ³H. Svensmark and L. M. Falicov, *Phys. Rev. B* **40**, 201 (1989).
- ⁴J. D. Axe, A. H. Moudden, D. Hohlwein, D. E. Cox, K. M. Mohanty, A. R. Moodenbaugh, and Youwen Xu, *Phys. Rev. Lett.* **62**, 2751 (1989).
- ⁵Z. Z. Wang, J. Clayhold, N. P. Ong, J. M. Tarascon, L. H. Greene, W. R. McKinnon, and G. W. Hull, *Phys. Rev. B* **36**, 7222 (1987).
- ⁶J. D. Jorgensen, M. A. Beno, D. G. Hinks, L. Soderholm, K. J. Volin, R. L. Hitterman, J. D. Grace, I. K. Schuller, C. U. Segre, K. Zhang, and M. S. Kleefisch, *Phys. Rev. B* **36**, 3608 (1987).
- ⁷G. Van Tendeloo, H. W. Zandbergen, and S. Amelinckx, *Solid State Commun.* **63**, 603 (1987).
- ⁸C. Chaillout, M. A. Alario-Franco, J. J. Capponi, J. Chenavas, P. Strobel, and M. Marezio, *Solid State Commun.* **65**, 283 (1988).
- ⁹M. A. Alario-Franco, J. J. Capponi, C. Chaillout, J. Chenavas, and M. Marezio, in *High-Temperature Superconductors*, edited by M. B. Brodsky, R. C. Dynes, K. Kitazawa, and H. L. Tuller (Materials Research Society, Pittsburgh, 1988).
- ¹⁰M. A. Alario-Franco, C. Chaillout, J. J. Capponi, J. Chenavas, and M. Marezio, *Physica C (Amsterdam)* **156**, 455 (1988).
- ¹¹J. L. Hodeau, P. Bordet, J. J. Capponi, C. Chaillout, and M. Marezio, *Physica C (Amsterdam)* **153-155**, 582 (1988).
- ¹²D. J. Werder, C. H. Chen, R. J. Cava, and B. Batlogg, *Phys. Rev. B* **37**, 2317 (1988).
- ¹³D. J. Werder, C. H. Chen, R. J. Cava, and B. Batlogg, *Phys. Rev. B* **38**, 5130 (1988).
- ¹⁴J. Reyes-Gasga, T. Kjekshus, G. Van Tendeloo, J. Van Landuyt, W. H. M. Bruggink, M. Verweij, and S. Amelinckx, *Solid State Commun.* **70**, 269 (1989).
- ¹⁵Y. Kubo, T. Ichihashi, T. Manako, K. Baba, J. Tabuchi, and H. Igarashi, *Phys. Rev. B* **37**, 7858 (1988).
- ¹⁶H. You, J. D. Axe, X. B. Kan, S. Hashimoto, S. C. Moss, J. Z. Liu, G. W. Crabtree, and D. J. Lam, *Phys. Rev. B* **38**, 9213 (1988).
- ¹⁷M. Tetenbaum, L. A. Curtiss, B. Tani, B. Czech, and M. Blander, *Physica C (Amsterdam)* **158**, 371 (1989).
- ¹⁸Y. Kubo and H. Igarashi, *Jpn. J. Appl. Phys. Pt. 2* **26**, L1988 (1987).
- ¹⁹L. T. Wille and D. de Fontaine, *Phys. Rev. B* **37**, 2227 (1988).
- ²⁰J. M. Sanchez, F. Mejía-Lira, and J. L. Morán-López, *Phys. Rev. B* **37**, 3678 (1988); J. M. Bell, *ibid.* **37**, 541 (1988).
- ²¹L. T. Wille, A. Berera, and D. de Fontaine, *Phys. Rev. Lett.* **60**, 1065 (1988).
- ²²L. T. Wille, *Phase Transitions* (to be published).
- ²³L. T. Wille, *Phys. Rev. B* **40**, 6941 (1989).
- ²⁴A. A. Aligia, A. G. Rojo, and B. Alascio, *Phys. Rev. B* **38**, 6604 (1988).
- ²⁵A. A. Aligia, A. G. Rojo, and B. Alascio, in *Progress in High Temperature Superconductivity*, edited by R. Nicolisky (World Scientific, Singapore, 1988), Vol. 9, p. 406.
- ²⁶A. G. Khachatryan and J. W. Morris, Jr., *Phys. Rev. Lett.* **61**, 215 (1988).
- ²⁷D. de Fontaine, M. E. Mann, and G. Ceder, *Phys. Rev. Lett.* **63**, 1300 (1989).
- ²⁸Zhi-Xiong Cai and S. D. Mahanti, *Phys. Rev. B* **40**, 6558 (1989); C. P. Burmester and L. T. Wille, *ibid.* **40**, 8795 (1989).
- ²⁹S. T. Chui, R. V. Kasowski, and W. Y. Hsu, *Phys. Rev. Lett.* **61**, 207 (1988).
- ³⁰A. Renault, J. K. Burdett, and J. P. Pouget, *J. Solid State Chem.* **71**, 587 (1987).
- ³¹M. H. Whangbo, M. Evain, M. A. Beno, V. Geiser, and J. M. Williams, *Inorg. Chem.* **27**, 467 (1988).
- ³²W. R. McKinnon, M. L. Post, L. S. Selwyn, G. Pleizier, J. M. Tarascon, P. Barboux, L. H. Greene, and G. W. Hull, *Phys. Rev. B* **38**, 6543 (1988).
- ³³J. Kondo, Y. Asai, and N. Nagai, *J. Phys. Soc. Jpn.* **57**, 4334 (1988).
- ³⁴L. F. Feiner and D. M. De Leeuw, *Solid State Commun.* **70**, 1165 (1989).
- ³⁵J. B. Torrance and R. M. Metzger, *Phys. Rev. Lett.* **63**, 1515 (1989).
- ³⁶H. Rushan, C. K. Chew, K. K. Phua, and Z. Z. Gan, *Phys. Rev. B* **39**, 9200 (1989).
- ³⁷A. K. McMahan, R. M. Martin, and S. Satpathy, *Phys. Rev. B* **38**, 6650 (1988).
- ³⁸M. S. Hybertsen, M. Schlüter, and N. E. Christensen, *Phys. Rev. B* **39**, 9028 (1989).
- ³⁹J. E. Hirsch, S. Tang, E. Loh, Jr., and D. J. Scalapino, *Phys. Rev. Lett.* **60**, 1668 (1988); *Physica C (Amsterdam)* **153-155**, 549 (1988); C. A. Balseiro, A. G. Rojo, E. R. Gagliano, and B.

- Alascio, Phys. Rev. B **38**, 9315 (1988); Physica C (Amsterdam) **153-155**, 1223 (1988); G. D. Mahan, Phys. Rev. B **40**, 2200 (1989); P. B. Littlewood, C. M. Varma, and E. Abrahams, Phys. Rev. Lett. **63**, 2602 (1989).
- ⁴⁰M. D. Núñez Regueiro and A. A. Aligia, Phys. Rev. Lett. **61**, 1889 (1988) [there is a mistake in the entry (a) of Table II, the factor $3(z-1)$ should be replaced by $2z-1$]; Int. J. Mod. Phys. B **2**, 899 (1988).
- ⁴¹A. A. Aligia, M. D. Núñez Regueiro, and E. Gagliano, Phys. Rev. B **40**, 4405 (1989).
- ⁴²A. A. Aligia, J. Garcés, and H. Bonadeo, Phys. Rev. B **42**, 10 266 (1990).
- ⁴³A. A. Aligia (unpublished).
- ⁴⁴Y. Tokura, J. B. Torrance, T. C. Huang, and A. I. Nazzari, Phys. Rev. B **38**, 7156 (1988).
- ⁴⁵S. Yamaguchi, K. Terabe, A. Imai, and Y. Iguchi, Jpn. J. Appl. Phys. Pt. 2 **27**, L220 (1988).
- ⁴⁶J. M. Tranquada, S. M. Heald, A. R. Moodenbaugh, and Y. Xu, Phys. Rev. B **38**, 8893 (1988).
- ⁴⁷A. A. Aligia and J. Garcés (unpublished).
- ⁴⁸J. A. Gardner, H. T. Su, A. G. McKale, S. S. Kao, L. L. Peng, W. H. Warnes, J. A. Sommers, K. Athreya, H. Franzen, and S.-J. Kim, Phys. Rev. B **38**, 11 317 (1988).
- ⁴⁹S. J. Rothman, J. L. Routbort, and J. E. Baker, Phys. Rev. B **40**, 8852 (1989).
- ⁵⁰J. M. Bassat, P. Odier, and F. Gervais, Phys. Rev. B **35**, 7126 (1987).
- ⁵¹C. H. Zhang, T. A. Callcott, K.-L. Tsang, D. L. Ederer, J. E. Blendell, C. W. Clark, T. Scimeca, and Y.-W. Liu, Phys. Rev. B **39**, 4796 (1989).
- ⁵²W. W. Warren, Jr., R. E. Walstedt, G. F. Brennert, R. J. Cava, B. Batlogg, and L. W. Rupp, Phys. Rev. B **39**, 831 (1989).
- ⁵³G. Bubeck, A. M. Oleś, and M. C. Böhm, Z. Phys. B **76**, 143 (1989), and references therein.
- ⁵⁴M. Kaburagi and J. Kanamori, Prog. Theor. Phys. **54**, 30 (1979).
- ⁵⁵S. M. Allen and J. W. Cahn, Acta Metall. **20**, 423 (1972).
- ⁵⁶(a) H. Bonadeo, Can. J. Phys. **62**, 904 (1984); (b) see also E. Ruch and D. J. Klein, Theor. Chim. Acta **63**, 447 (1983).
- ⁵⁷M. Tinkham, *Introduction to Superconductivity* (McGraw-Hill, New York, 1975), p. 149.
- ⁵⁸Y. Y. Wang, R. Rammal, and B. Pannetier, J. Low Temp. Phys. **68**, 301 (1987).
- ⁵⁹M. Kogachi, S. Nakanishi, K. Nakahigashi, S. Minamigawa, H. Sasakura, N. Fukuoka, and A. Yanase, Jpn. J. Appl. Phys. Pt. 2 **27**, L1228 (1988).
- ⁶⁰H. Oyanagi, H. Ihara, T. Matsubara, T. Matsushita, M. Hirabayashi, M. Tokumoto, K. Murata, N. Terada, K. Senzaki, T. Yao, H. Iwasaki, and Y. Kimura, Jpn. J. Appl. Phys. Pt. 2 **26**, L1233 (1987).
- ⁶¹K. Kishio, J. Shimoyama, T. Hasegawa, K. Kitazawa, and K. Fueki, Jpn. J. Appl. Phys. Pt. 2 **26**, L1228 (1987).
- ⁶²S. Yamaguchi, K. Terabe, A. Saito, S. Yahagi, and Y. Iguchi, Jpn. J. Appl. Phys. Pt. 2 **27**, L179 (1988).
- ⁶³N. C. Yeh, K. N. Tu, S. I. Park, and C. C. Tsuei, Phys. Rev. B **38**, 7087 (1988).
- ⁶⁴K. F. McCarty, J. C. Hamilton, R. N. Shelton, and D. S. Ginley, Phys. Rev. B **38**, 2914 (1988).
- ⁶⁵A. G. Khachatryan and J. W. Morris, Jr., Phys. Rev. Lett. **64**, 76 (1990).
- ⁶⁶A. A. Aligia and C. I. Ventura, Solid State Commun. (to be published).
- ⁶⁷H. Strauven, J. P. Locquet, O. B. Verbeke, and Y. Bruynseraede, Solid State Commun. **65**, 293 (1988).
- ⁶⁸P. Monod, M. Ribault, F. D'Yvoire, J. Jegoudez, G. Collin, and A. Revcolevschi, J. Phys. (Paris) **48**, 1369 (1987).
- ⁶⁹H. Shaked, J. D. Jorgensen, J. Faber, Jr., D. G. Hinks, and B. Dabrowski, Phys. Rev. B **39**, 7363 (1989).
- ⁷⁰R. Beyers, B. T. Ahn, G. Gorman, V. Y. Lee, S. S. Parkin, M. L. Ramirez, K. P. Roche, J. E. Vazquez, T. M. Gür, and R. A. Huggins, Nature (London) **340**, 619 (1989).